https://doi.org/10.1016/j.trd.2021.102949 

# Assessing Carbon Dioxide Emissions of High-Speed Rail: The Case of Beijing-Shanghai Corridor

Peihong Chen[1]*, Yuan Lu[1], Yulai Wan[2], Anming Zhang[3]

[1] School of Economics and Management, Beijing Jiaotong University, Beijing, China

[2] Department of Logistics and Maritime Study, Hong Kong Polytechnic University, Hong Kong

[3] Sauder School of Business, University of British Columbia, Vancouver, BC, Canada

* Corresponding author: phchen@bjtu.edu.cn

February 2021; Revised May 2021

## Abstract

This paper provides an ex-post assessment of net carbon dioxide (CO2) emissions of the Beijing-Shanghai high-speed rail (HSR) by including both mode substitution and traffic generation effects with a life-cycle approach. We are among the first authors to examine the emissions effects of a long-haul HSR and to consider the effects of avoided infrastructure expansion and vehicle manufacturing due to traffic diversion. We find that avoided infrastructure expansion plays a limited role in offsetting CO2 emissions from the construction of an HSR infrastructure, but the reduced demand for passenger vehicles can offset a larger share of emissions from the manufacturing of HSR rolling stock. Initially, too much traffic was diverted from ordinary-speed rail (OSR) to HSR, increasing emissions at the operation stage. As traffic diverted from road and air increased, the net emissions at the operation stage turned negative, offsetting emissions from infrastructure construction and vehicle manufacturing.

**Keywords:** High-speed rail; Carbon dioxide emissions; Mode substitution; Life-cycle assessment

## 1. Introduction

While transportation plays a crucial role in human mobility and economic development, its harmful environmental effects attributed to climate change have received considerable attention in public debate. According to Sims et al. (2014), transportation sector produced about 23% energy-related CO2 emissions in 2010 and without aggressive mitigation measures, transport-related CO2 emissions could more than double by 2050 and even triple by 2100. Modal substitution towards the low-carbon transportation modes is one mitigation strategy with high potential (Sims et al., 2014). It is widely considered that public transport systems, such as railways, are more environmentally friendly than private automobiles (Gursoy et al., 2020). As a major public transportation mode, high-speed rail (HSR) can have an important implication for the environment. In September 2020, at the 75th UN General Assembly, China put forward the goal of reaching carbon peak by 2030 and carbon neutral by 2060, which makes the issue relevant in the Chinese context, given that China is the No.1 emitter and has by far the largest HSR network in the world.

HSR may affect environment at the construction stage as well as the operation stage, while the latter is largely associated with its impact on passengers' intercity travel behavior and hence traffic-related emissions. The traffic impact of HSR is two-fold. Since HSR offers shorter travel time and possibly higher service quality, it may attract passengers away from other transportation modes in the inter-city passenger market. Such substitution effect may occur not only in public transport but also in private mode. Many studies have reported a demand shift from ordinary trains, air flights, intercity coaches and private cars to HSR (e.g., Givoni and Dobruszkes, 2013; Lee et al., 2004; Li et al., 2020). HSR has a competitive advantage over highway and air transportation especially in the medium- to long-range travel sector (e.g., Wang et al., 2018; Lawrence et al., 2019).[1] This traffic diversion effect is generally considered as environmental friendly, because among various modes of transport, such as HSR, coaches, cars and aircraft, HSR is found to have the lowest emissions under the ideal passenger density given a particular origin-destination pair (Baumeister, 2019; Dalkic et al., 2017) and the lowest greenhouse gas (GHG) emissions per passenger-km (p-km) travelled based on the life-cycle approach (Chester and Horvath, 2012). This is especially the case if HSR can divert traffic from air and automobiles which emit the most on the per-passenger basis. However, the introduction of a new transportation mode or an improvement in transportation systems can

[1] Of course, HSR is not competitive vs. air transportation in the very long-distance travel (see, e.g., Zhang et al., 2019, for a recent literature survey).

induce people to take more trips. Such induced (generated) traffic has also been observed in various HSR lines (see Givoni and Dobruszkes, 2013, for a comprehensive review). Although generated traffic can be economically beneficial, it produces extra emissions and can offset the environmental benefit of the mode substitution effect mentioned above.

In other words, to assess the carbon dioxide (CO2) emissions impacts of an HSR project, in addition to the widely applied life-cycle approach which mainly focuses on HSR alone, we need to consider both the mode substitution and traffic generation effects. Thus, in this paper, we conduct a counterfactual assessment of the CO2 emissions impacts of the Beijing-Shanghai (B-S) HSR line in China. In the analysis, we identify both mode substitution effect and traffic generation effect by comparing the actual traffic with HSR and the projected traffic without HSR. Then, we assess these two effects' net impact on the carbon footprint.

We contribute to the literature in the following ways. First, most published works of this stream conduct ex-ante assessment with predicted traffic data or assumed level of modal shift. Our study is an ex-post assessment based on actual traffic data. Second, almost all the published works in this stream focus on the European context where HSR lines mainly serve in short-haul markets (less than 500 km). In these short-haul markets, HSR mainly causes modal shift from other ground modes, as air transport has limited presence in these markets. In medium/long-haul markets, however, air is likely to be the dominant mode before the entry of HSR and ex-post modal shift from air to HSR can be much stronger than the other ground modes. The B-S HSR line has a total length of 1318 km, a designed maximum speed of 380 km/h and 24 stations. Such a long distance allows the B-S HSR to serve short-haul, medium-haul and long-haul city-pair markets. In fact, the fastest HSR service between Shanghai and Beijing only takes about four hours while a flight between these two cities takes over two hours. Considering the lengthy check-in and boarding process of a flight, HSR is very competitive in this long-haul route. Therefore, a case study based on the B-S HSR line may provide some unique value. Finally and most importantly, when assessing the avoided emissions due to the mode substitution effect, the existing studies only take into account avoided emissions from vehicles and ignore the fact that the emissions from infrastructure construction and vehicle manufacturing in air, road and conventional rail transport will be reduced as well. In our study, the mode substitution effect covers traffic diversion from air, ordinary train and road transport to HSR, as well as its consequential reduction in the need for building extra infrastructure and producing extra vehicles for those transportation modes to satisfy future travel demand.

This paper is organized as into 6 sections. Section 2 provides literature reviews on different approaches on assessing the carbon emissions impacts of HSR. Section 3 introduces the framework that we use to assess CO2 emissions. Sections 4 to 6 provide detailed calculation of net CO2 emissions from each life-cycle stage. Section 7 presents the lifetime net CO2 emissions by summarizing results from Sections 4 to 6. Section 8 provides the findings and conclusions from our research.

## 2. Literature Review

To assess the carbon emissions effects of HSR, three approaches are widely applied in the literature. The first approach is to compare the amount of CO2 or CO2-equivalent (CO2-eq) generated by various transportation modes to move one passenger in a certain route market. A typical example is a study conducted by Baumeister (2019) which covers 16 city-pair markets linking to Helsinki Airport or the city of Helsinki in Finland. In each city-pair market, Baumeister (2019) compared the per-passenger CO2-eq emissions across various modes of transport, including air, train, car and coach, and found that in all route markets trains produce the least amount of CO2-eq per passenger while airplanes emit the most. Hagedom and Sieg (2019) exemplify a variation of this approach. They argue that given a fixed full price which is the sum of ticket price and time cost, the choice of transportation mode can affect leisure travelers' decision on the travel distance. Therefore, instead of considering a given route, they compare emissions from different modes of transport with a given full price. As studies in this stream mainly focus on one single trip of an individual traveler, they consider neither the actual traffic volume of each transportation mode nor the mode substitution effect and traffic generation effect of HSR. In addition, emissions from infrastructure construction and vehicle manufacturing are abstracted away as well. As a result, this approach cannot be used to assess the overall emissions impacts of developing HSR, but it may be applied to produce inputs, such as per-passenger emissions figures of certain routes, for the other two streams of studies.

The second approach focuses on measuring energy consumption and emissions throughout the lifespan of an HSR project. This stream of studies mainly applies the Life cycle assessment (LCA) method which assesses environmental effects in several stages of an HSR project, including roughly infrastructure construction and operation, rolling stock manufacturing, and train operation and maintenance. The main objective of those studies is to identify the major sources and stages of emissions and energy consumption. There can be some variation in the division of stages across different studies. For example, Baron et al. (2011) considers four stages, i.e., conception, construction, operation and disposal, and they find that an HSR project's $CO_2$ emissions mostly comes from operation, followed by construction, while conception and disposal accounts for a very small proportion. Due to the large variation in technology, standards and energy sources, the estimated environmental effects can vary significantly across countries and HSR lines.

In the context of China, LCA of its HSR lines has emerged recently. Yue et al. (2015) provide a very comprehensive and detailed calculation of environmental effects of the B-S HSR line, including not only GHG emissions, but emissions of PM2.5, fossil resource depletion, Eutrophication potential of surface water, etc. They find that train operation contributes to 86% of the life cycle greenhouse gas emissions, which is similar to an LCA study of the proposed California HSR (Chester and Horvath, 2010). However, another LCA study on the B-S HSR line conducted by Kaewunruen et al. (2019) finds that 64.86% of the carbon emissions and 54.31% of energy consumption are from the construction stage, while the operation and maintenance stage only accounts for 31.60% and 35.32% respectively. This huge difference in the findings of Yue et al. (2015) and Kaewunruen et al. (2019) mainly stems from the exclusion of train operation and maintenance in the latter study, as Kaewunruen et al. only includes infrastructure operation and track maintenance in the operation and maintenance stage. Chang et al. (2019) apply a process-based input-output (IO) life-cycle inventory (LCI) approach to estimate energy consumption and emissions of $SO_2$, PM2.5 and greenhouse gas of the Beijing-Shijiazhuang HSR. This approach involves assessing not only emissions directly associated with constructing of infrastructure and manufacturing of vehicles, but also emissions indirectly associated with producing inputs used to build HSR and vehicles, i.e. the emissions throughout the supply chains of materials and fuel. A similar approach was applied by Cheng (2020) to assess embodied carbon emissions, water consumption, land occupation and embodied raw material use due to the construction of the Beijing-Tianjin intercity HSR. One contribution of Cheng (2020) is to include carbon emissions from the construction of HSR stations into the analysis, which is missing in Chang et al.'s study. Although Chang et al. (2019) and Cheng (2020) include both direct and indirect emissions, in our study, we mainly apply HSR $CO_2$ emissions rates estimated by Baron et al. (2011) for infrastructure construction and vehicle manufacturing stages, because Baron et al. provide the most complete emission-related information for all the components of HSR infrastructure, including not only tracks, but also tunnels and stations. Moreover, Baron et al. estimated emissions rates of several HSR lines in China, making it possible to cross check the accuracy of the estimations.

Overall, most LCA studies deal with the complexity of calculating environmental effects of HSR projects per se and pay less attention to the interaction between HSR and other modes of transport. In fact, none of the abovementioned studies of Chinese HSR lines consider mode substitution and traffic generation effects, despite that there can be a comparison of carbon emissions per p-km across different modes (e.g. Chang et al., 2019). Some LCA studies may briefly discuss avoided emissions due to the introduction of HSR and hence the traffic reduction of other transportation modes, such as road and air. One may refer to Baron et al. (2011) for a case study in South France and Chang and Kendall (2011) for a case study in California, USA. However, those brief analyses are usually based on strong assumptions in modal shift as well as HSR traffic volume throughout its lifespan, and most importantly fails to consider the traffic generation effect of HSR.

The third stream of studies originates from the counterfactual environmental cost-benefit analysis of an HSR project. The main feature of this approach is to compare emissions in the scenario with HSR and the scenario without HSR by assessing both mode substitution and traffic generation effects. As most LCA studies suggest the operation stage accounts for the highest share of carbon emissions of an HSR project, earlier studies in the third stream ignored infrastructure construction and rolling stock manufacturing stages, while focused on the train operation stage only (e.g. Dalkic et al., 2017; Westin and Kageson, 2012). To better measure the environmental impacts of HSR, the recent trend is to include HSR infrastructure construction and rolling stock manufacturing stages in the analysis by incorporating features of LCA studies (e.g. Akerman, 2011; Bueno et al., 2017).

However, we identify several limitations in the existing studies of this stream. First, to our knowledge, all the studies only include avoided emissions in the operation stage due to the mode substitution effect. In fact, as some road or air traffic is diverted to HSR, the demand for constructing new roads or airports and manufacturing vehicles and aircraft is reduced. Thus, the vehicle manufacturing and the infrastructure construction of the other non-HSR modes should also be considered when assessing the avoided emissions. Second, many studies in this stream conducted ex-ante assessment for a proposed or hypothetical HSR project using projected or assumed traffic volumes (e.g. Akerman, 2011; Bueno et al., 2017; Westin and Kageson, 2012). To our knowledge, Dalkic et al. (2017) is the only ex-post study using actual traffic data together with passenger surveys to derive diverted traffic from other modes and induced traffic due to the introduction of HSR. Ex-post evaluation based on the actual traffic volume is supposed to be more accurate. Third, almost all the studies are conducted in the context of Europe where HSR lines serve short-haul markets. For example, Akerman (2011) studies two HSR links, one 440 km link from Stockholm (Järna) to Gothenburg via Jönköping and one 300 km link from Jönköping to Malmö/Copenhagen. Bueno et al. (2017) studies a projected Y-shaped HSR network in Spain with a total length of 180 km. Dalkic et al. (2017) includes two HSR links in Turkey, the Ankara-Eskisehir link with 245 km and the Ankara-Konya link with 306 km. In these short-haul markets, HSR tends to impose a stronger mode substitution effect with other ground transport, such as conventional rail, buses and cars, while having less interaction with air transport which has the highest carbon emissions rate among all transportation modes. As a result, many of those studies find that HSR's carbon reduction performance is limited.

As the mode substitution and traffic generation effects are the focus of this paper, we will apply the third approach with a life-cycle perspective and fill in the research gaps listed above. We conduct an ex-post evaluation of $CO_2$ emissions effects of the B-S HSR project in China with actual traffic data. This HSR line has a length of 1318 km and the minimum HSR travel time between the endpoint cities, i.e. Beijing and Shanghai, is just slightly over 4 hours. Thus, our study will add new knowledge about the environmental effects of long-haul HSR lines to the literature. Moreover, to better estimate avoided emissions, we also take into account avoided infrastructure and vehicles of other transportation modes as a large amount of traffic is diverted to HSR.

Finally, our study and all the above-mentioned studies only assess $CO_2$ emissions from transportation sectors directly affected by the entry of HSR. In the literature, we observe a couple of papers applying the computational general equilibrium (CGE) models, which establish the linkage between transportation and the entire economy and hence assesses the change in $CO_2$ emissions from transportation as well as all the other sectors in the economy as certain policies cause traffic diversion among transportation modes. For example, Cristea et al. (2013) study the impact of tariff reduction in international trade on the redistribution of trade flows and in turn the emissions from international transportation of physical goods and its share in global $CO_2$ emissions. Avetisyan (2018) studies the impacts of GHG tax on choice of transportation mode in international trade and hence emissions from international transport of physical goods. While the CGE approach provides a more comprehensive assessment by including all sectors in the economy, it is difficult to be directly applied in the context of HSR, because HSR primarily affects the domestic passenger sector with some indirect impacts on freight sector by probably releasing the capacity of conventional rail infrastructure. The linkage between the introduction of HSR and entire economy is a lot more complex and in fact the relationship between passenger travel and other non-transportation sectors is not as straightforward as the relationship between international transport and international trade. For example, the entry of HSR may affect urban development, location of labor, and location of consumption and manufacturing sites as people move to other cities (e.g., Liu et al., 2020; Zhou and Zhang, 2021). However, it is unclear how and to what extent such change could happen and there lacks sufficient data to build models which incorporate these complex relationships. One may refer to Zhang et al. (2019) for a comprehensive review on the debate of HSR's impact on economic development. Therefore, following the practice of most HSR-related studies in the transportation literature, we only focus on the major life-cycle stages of the transportation sector.

## 3. Evaluation Framework of CO2 Emissions

### 3.1 The B-S corridor and B-S HSR

In the 1990s, the Beijing-Shanghai ordinary-speed railway (B-S OSR) was the busiest transportation trunk line in China, with the capacity utilization rate of the whole line reaching 98-100%. There was an obvious mismatch between high transportation demand and limited capacity, and hence it was believed that constructing a passenger-dedicated HSR line parallel to the B-S OSR would be the best way to expand the transportation capacity of the Beijing-Shanghai corridor (B-S corridor) (Figure 1). This B-S HSR could not only meet the growing demand of passenger transport and improve the quality of passenger service, but also release the capacity of the B-S OSR to accommodate more freight trains.


Figure 1 Beijing-Shanghai transportation corridor

The construction of the B-S HSR began on April 18, 2008, and the entire line started commercial service on June 30, 2011. The B-S HSR has 24 stations and a total length of 1318 km with a designed maximum speed of 380 km/h and operating speed of 350 km/h. It is designed to accommodate 160 pairs of trains per day and move 160 million passengers per year in two directions. The passenger traffic volume and the number of train journeys operated increased rapidly from 2011 to 2017 (Table 1) and both have exceeded the designed volume since 2017. The average occupancy rate of seats provided on this line was 75% in the 2011-2017 period. The B-S HSR has become the busiest HSR line in China and its traffic density has grown closer to the level of Japan's Tokaido Shinkansen within just 6.5 years (Table 2). The latter has been in operation for nearly half a century before reaching the world's highest traffic density. According to the Medium-and Long-Term Railway Network Planning (2016) of China, over ten HSR lines connect with the B-S HSR, which will feed more traffic to the B-S HSR in the future. Thus, the traffic density of B-S HSR is expected to grow further and is likely to surpass that of the Tokaido Shinkansen in the future.

Table 1 Traffic volume of B-S HSR from 2011 to 2017

| Year | 2011 | 2012 | 2013 | 2014 | 2015 | 2016 | 2017 |
|---|---|---|---|---|---|---|---|
| Number of train journeys operated | 26493 | 64126 | 72240 | 94635 | 110062 | 137419 | 159201 |
| Passenger volume (million persons) | 24.5 | 65.1 | 83.9 | 105.9 | 122.4 | 151.8 | 179.0 |
| Growth rate of passenger volume | --- | 34.5% | 29.3% | 26.2% | 15.3% | 23.7% | 18.2% |
| Load factor | 69.9% | 67.7% | 76.0% | 76.5% | 76.5% | 76.1% | 73.1% |

Data source: Prospectus of Beijing-Shanghai HSR Co., Ltd

Table 2 Traffic densities of B-S HSR and Tokaido Shinkansen

| Year | B-S HSR | | Tokaido Shinkansen | |
|---|---|---|---|---|
| | Passenger turnover (billion p-km) | Traffic density (billion p-km / km) | Passenger turnover (billion p-km) | Traffic density (billion p-km / km) |
| 2011 | 16.17 | 0.01 | 44.30 | 0.09 |
| 2012 | 42.65 | 0.03 | 46.93 | 0.09 |
| 2013 | 54.13 | 0.04 | 48.87 | 0.09 |
| 2014 | 76.76 | 0.06 | 50.13 | 0.10 |
| 2015 | 93.44 | 0.07 | 52.17 | 0.10 |
| 2016 | 111.60 | 0.08 | 52.91 | 0.10 |
| 2017 | 137.13 | 0.10 | 54.76 | 0.11 |

Note: Traffic density = Passenger turnover / Line length

Data source: Beijing-Shanghai HSR Co., LTD., Central Japan Railway Company

The inauguration of B-S HSR has different impacts on other transportation modes along the B-S corridor, including B-S OSR, air transport and expressways. The B-S OSR is a passenger and freight dual-purpose electrified railway with 148 stations and a total length of 1463 km. After several upgrades, the maximum operating speed of the passenger trains has reached 80-160 km/h since 2007. The passenger volume of B-S OSR reduced by over 37%, comparing with the 2010 figure, right after the commencement of the B-S HSR in 2011 (Table 3). The passenger volume of B-S OSR further dropped in 2012, and then gradually reached stability and maintained at around 55 million passengers per year. This is mainly because of the different market segments served by HSR and OSR, as OSR is cheaper and can stop at smaller stations.

Table 3 Traffic volume of B-S OSR from 2010 to 2017

| Year | 2010 | 2011 | 2012 | 2013 | 2014 | 2015 | 2016 | 2017 |
|---|---|---|---|---|---|---|---|---|
| Passenger volume (million persons) | 90.4 | 56.6 | 47.9 | 52.6 | 56.7 | 55.2 | 54.1 | 54.7 |
| Passenger turnover (billion p-km) | 44.06 | 34.38 | 29.51 | 31.16 | 33.68 | 32.10 | 31.97 | 32.23 |

Data source: CR Beijing, CR Jinan and CR Shanghai [2]

The expressways' passenger flow density along the major sections of the B-S corridor is shown in Table 4. Although the B-S HSR has diverted some expressway traffic, almost all the expressway sections have experienced traffic growth during the 2010-2017 period, except for the Beijing-Tianjing and Tianjing-Dezhou sections. However, the growth became slower after the entry of B-S HSR.

Table 4 Expressway passenger flow density in B-S corridor (million p-km/km)

| Section | 2010 | 2017 | Average annual growth rate (%) |
|---|---|---|---|
| Beijing-Tianjin | 24.10 | 23.29 | -3.40 |
| Tianjin -Dezhou | 20.51 | 20.49 | -0.10 |
| Dezhou -Jinan | 15.41 | 21.38 | 5.61 |
| Jinan - Yanzhou | 21.89 | 28.53 | 4.51 |
| Yanzhou -Xuzhou | 10.04 | 13.69 | 5.30 |
| Xuzhou -Bengbu | 10.51 | 16.62 | 7.94 |
| Bengbu -Nanjing | 22.76 | 39.10 | 9.44 |
| Nanjing-Changzhou | 55.59 | 96.77 | 9.66 |
| Changzhou-Shanghai | 76.68 | 104.59 | 5.31 |

Data source: Statistical Analysis Report of China's Expressway Traffic Volume Survey (2010-2017) conducted by Transportation Science Research Institute of Chang'an University

Air routes serving city-pairs along the B-S corridor were heavily affected by the B-S HSR. In particular, Beijing-Xuzhou and Nanjing-Tianjin routes ceased operation in 2012,

[2] The B-S OSR belongs to three different railway companies, namely China Railway Beijing Group Co., Ltd (CR Beijing), China Railway Jinan Group Co., Ltd (CR Jinan) and China Railway Shanghai Group Co., Ltd (CR Shanghai).

Beijing-Jinan route ceased operation in 2013, Beijing-Changzhou route ceased operation in 2014, and Beijing-Wuxi and Shanghai-Jinan routes ceased operation in 2015. Only three long-haul routes remain operation in 2017, namely Beijing-Shanghai, Beijing-Nanjing and Tianjin-Shanghai routes. Despite the strong substitution effect of B-S HSR on parallel air routes, the passenger throughput of airports in cities along the B-S corridor is still growing (Table 5). In fact, except for Beijing and Shanghai, all the other airports achieved over 10% average annual growth rate during the 2010-2017 period, suggesting that air routes that do not directly compete with the B-S HSR might have experienced substantial growth.

Table 5 Passenger throughput of airports in the B-S corridor (million persons)

| City | 2010 | 2017 | Average annual growth rate (%) |
|---|---|---|---|
| Beijing | 76.09 | 101.74 | 4.24 |
| Shanghai | 71.88 | 111.89 | 6.53 |
| Tianjin | 7.28 | 21.01 | 16.35 |
| Nanjing | 12.53 | 25.82 | 10.88 |
| Jinan | 6.90 | 14.32 | 11.00 |
| Xuzhou | 0.66 | 1.92 | 16.50 |
| Changzhou | 0.66 | 2.51 | 21.08 |
| Wuxi | 2.54 | 6.68 | 14.85 |

Data source: "Statistical data on civil aviation of China" (2010-2017), by Civil Aviation Administration of China (CAAC).

### 3.2 Diverted and generated traffic

As mentioned in the introduction, the $CO_2$ emissions effects of HSR are associated with both mode substitution and traffic generation effects, before assessing the emissions effects, we first estimate the amount of traffic diverted to HSR from other potential transportation modes and the amount of induced HSR traffic from 2011 to 2017 annually.

The amount of HSR traffic diverted from transportation mode *i* (i=1, road; i=2, air; i=3, OSR) is the difference between mode *i*'s actual traffic after the entry of HSR and the projected traffic as if HSR were not introduced. In general, let $Q_{i0}$ be the projected traffic volume of mode *i* as if the B-S HSR were not in operation, let $Q_{i1}$ be the actual traffic volume of mode *i* with the operation of the B-S HSR, and let $t_0$ be the point of time when HSR enters the market. Then, the diverted traffic of mode $i$, $Q_i$, in year *t* ($t \geq t_0$) can be written as

$$Q_i(t) = Q_{i0}(t) - Q_{i1}(t) \tag{1}$$

The projected traffic in the hypothetical scenario of no HSR entry, i.e., $Q_{i0}(t)$ where $t \geq t_0$, is obtained by establishing a trend growth model using historical data before the commencement of HSR operation. That is, using historical traffic data of mode *i*, we establish a functional relationship between actual historical traffic data ($Q_{ia}$) and time ($t$), $Q_{ia}(t)$

where $t < t_0$, by regressing traffic data on certain transformation of time variable. Such transformation of time variable can be in a linear form, a quadratic form, a natural log, or an exponential form, depending on the observed pattern of traffic data over time. Then, we assume that this time series pattern will continue after $t_0$ if there were no HSR entry and thus the projected traffic without HSR entry after $t_0$ will be $Q_{i0}(t) = Q_{ia}(t)$ for $t \geq t_0$. One may refer to Sun et al. (2018) for detailed calibration of the trend growth model for each transportation mode and each section along the B-S corridor. Taking road transport as an example, we use the actual traffic volume of B-S Expressway from 2004 to 2010, during which the B-S HSR did not exist, to fit a trend growth model of road traffic. Then, this growth model is used to predict the trend traffic volume of the B-S Expressway from 2011 to 2017, as shown by the dotted line in Figure 2. As this growth model is applied by assuming there were no HSR entry in the 2011-2017 period, this trend traffic volume is the projected road traffic as if HSR were not introduced. The excess of the projected traffic over the actual traffic after the entry of HSR (2011-2017 period) is the estimated traffic that diverted from road to HSR[3]. In the same way, the traffic of HSR diverted from OSR and air can be calculated. The actual calculation is a bit more complicated than the above brief description since certain segments of the B-S HSR line started operation before the final completion of the entire B-S HSR line, which requires some extra adjustments as specified by Sun et al. (2018) in detail.

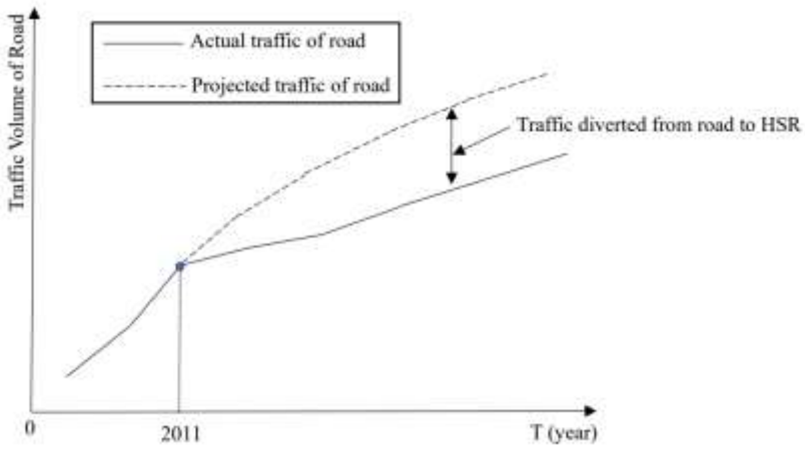


Figure 2 Illustration of the estimation of diverted traffic from road to HSR

The generated HSR traffic, $Q_G$, is the difference between actual HSR traffic of the B-S

[3] Due to the difficulty in obtaining the statistical data, only the traffic volume diverted from B-S expressway is considered here, and the traffic volume diverted from provincial and county roads in B-S corridor is not considered. Thus, the total traffic volume diverted from road to B-S HSR is underestimated to a certain extent while the net CO2 emissions tends to be overestimated as diverting traffic from road to HSR is likely to reduce emissions.

HSR line, $Q_h$, and the sum of diverted traffic across all non-HSR modes, as indicated in equation (2).

$$Q_G(\mathrm{t}) = Q_h(\mathrm{t}) - \sum_i Q_i(t) \quad (2)$$

In this paper, we use data from various sources. The actual passenger number of HSR is obtained from the annual report of Beijing-Shanghai HSR Co., Ltd. The OSR passenger number is obtained from CR Beijing, CR Jinan and CR Shanghai. The road traffic data comes from the Statistical Analysis Report of China's Expressway Traffic Volume Survey (2011-2017). The air passenger data is taken from the Statistical Data on Civil Aviation of China (2011-2017). The only available data of expressway traffic in China is passenger traffic density, instead of origin-destination (OD) traffic volume. To resolve this problem, we utilize the feature that the distance of an average passenger highway journey is 99.9975 km[4], about 100 km in China and divide the expressway into several sections, each with a length of about 100 km. By assuming each section as one OD market, the passenger flow density of each expressway section can be approximately considered as OD passenger traffic. As a result, the B-S expressway is divided into nine sections. Then, we adjust the traffic data of the other modes so that they can be comparable to the nine expressway sections. In particular, the traffic volumes of the 23 sections of the B-S HSR are also merged into those nine sections defined for the expressway. The traffic volumes of the 11 affected air routes are also rearranged into nine city-pairs accordingly. Then, in our study, the diverted and generated traffic volumes are calculated based on the nine sections from 2011 to 2017 annually. The total amount of diverted traffic and generated traffic are presented in Table 6 while the detailed traffic diversion and generation of each section are provided in Appendix A.

As shown in Table 6, the diverted traffic from OSR, road and air contribute to majority of the HSR traffic. From 2011 to 2017, on average, the diverted traffic from OSR accounted for 41.55% of the HSR traffic volume, that from road accounted for 37.19%, and that from air accounted for 3.92%, while the generated traffic only accounted for 17.34%. The traffic composition of the B-S HSR is representative in China. According to the World Bank report (2019), 80% - 90% of HSR traffic is diverted from other modes (OSR, road and air), and 10-20% of the traffic is newly generated in the corridors in China.

[4] The data is referred to Statistical Analysis Report of China's Expressway Traffic Volume Survey 2017.

Table 6 Total diverted and generated traffic of B-S HSR from 2011 to 2017

| Year | | 2011 | 2012 | 2013 | 2014 | 2015 | 2016 | 2017 | Average |
|---|---|---|---|---|---|---|---|---|---|
| Traffic Volume (million persons) | Diverted from OSR | 58.84 | 74.66 | 70.64 | 67.70 | 71.82 | 75.71 | 76.63 | 77.00 |
| | Diverted from road | 30.05 | 46.43 | 47.61 | 66.48 | 63.67 | 86.55 | 121.70 | 68.93 |
| | Diverted from air | 1.97 | 5.06 | 6.64 | 7.84 | 8.88 | 9.75 | 10.77 | 7.27 |
| | Generated | 3.63 | 9.85 | 32.12 | 39.45 | 51.22 | 46.66 | 33.50 | 32.13 |
| | Total | 94.49 | 136.00 | 157.01 | 181.47 | 196.57 | 218.67 | 242.60 | 185.34 |
| Proportion of HSR traffic (%) | Diverted from OSR | 62.27 | 54.90 | 44.99 | 37.31 | 36.54 | 34.62 | 31.59 | 41.55 |
| | Diverted from road | 31.80 | 34.14 | 30.32 | 36.63 | 32.39 | 39.58 | 50.16 | 37.19 |
| | Diverted from air | 2.08 | 3.72 | 4.23 | 4.32 | 4.52 | 4.46 | 4.44 | 3.92 |
| | Generated | 3.84 | 7.24 | 20.46 | 21.74 | 26.56 | 21.34 | 13.81 | 17.34 |
| | Total | 100.00 | 100.00 | 100.00 | 100.00 | 100.00 | 100.00 | 100.00 | 100.00 |

### 3.3 Emissions assessment model

To evaluate the $CO_2$ emissions effects of the B-S HSR project, a simplified life-cycle assessment (LCA) is adopted. The life cycle of an HSR project includes four phases: conception, construction, operation and disposal (Baron et al., 2011). Since the $CO_2$ emissions from conception and disposal accounts for a very small proportion, in this study we ignore these two phases and only consider the construction and operation stages, including infrastructure construction, vehicle manufacturing and vehicle operation. Due to the diversity of infrastructure and vehicle maintenance cycles of four modes of transportation, the $CO_2$ emissions from maintenance are aggregated into the emissions from infrastructure construction and vehicle manufacturing to simplify the calculation. However, the $CO_2$ emissions from infrastructure operations (such as air conditioning and lighting of station buildings) are excluded.

The construction of new transportation infrastructure and the manufacturing and operation of associated vehicles would emit extra GHG, while the operation of the new transportation service may reduce the usage and hence emissions of all the other transportation modes serving the same market. Thus, the net $CO_2$ emissions of an HSR infrastructure should be assessed by comparing $CO_2$ emissions of all relevant transportation modes in two alternative scenarios, one without the HSR and the other with the HSR (Bueno et al., 2017), assuming all the other factors keep constant. Thus, the net $CO_2$ emissions (*NCE*) of a new HSR project at year *t* would be

$$NCE(t) = CE_1(t) - CE_0(t) \tag{3}$$

Where $CE_1$ represents $CO_2$ emissions from all transportation modes when the HSR exists, while $CE_0$ is $CO_2$ emissions from all transportation modes when the HSR does not exist. *NCE* can be further divided into net emissions derived from infrastructure construction ($NCE_c$), vehicle manufacturing ($NCE_m$) and vehicle operation ($NCE_o$), respectively.

$$NCE(t) = NCE_c(t) + NCE_m(t) + NCE_o(t) \tag{4}$$

While infrastructure construction occurs only once before the operation, vehicle manufacturing can occur several times and vehicle operation occurs every year during the whole life cycle of the infrastructure. Here, $NCE_c(t)$ and $NCE_m(t)$ are annualized net emissions which are obtained by evenly allocating generated emissions across the lifespan of the infrastructure and vehicles.

The net emissions derived from infrastructure construction can be defined as the difference of $CO_2$ emissions from infrastructure construction with and without HSR, i.e.

$NCE_c(t) = CE_{c1}(t) - CE_{c0}(t)$. Although all non-HSR transportation modes may require infrastructure expansion to accommodate growing travel demand, comparing with infrastructure construction in the "without HSR" scenario, the main difference of the "with HSR" scenario is the extra $CO_2$ emissions from constructing HSR and the avoided construction of the other modes' infrastructure associated to traffic diversion from those modes to HSR. Therefore, $NCE_c$ can be written as

$$NCE_c(t) = CE_c^H(t) - \sum_i CE_c^i(t) \quad (5)$$

Where $CE_c^H(t)$ is the actual $CO_2$ emissions from the construction of HSR infrastructure in year *t*, and $CE_c^i(t)$ is the avoided $CO_2$ emissions as fewer infrastructure expansion projects are needed for transportation mode i (i = air, road and OSR) in the "with HSR" scenario than the "without HSR" scenario. The calculation of $CE_c^H$, $CE_c^i$ and $NCE_c$ is provided in Section 4.

Similarly, the net emissions derived from vehicle manufacturing can be written as

$$NCE_m(t) = CE_m^H(t) - \sum_i CE_m^i(t) \quad (6)$$

Where $CE_m^H(t)$ is the actual $CO_2$ emissions from the manufacturing of HSR rolling stocks in year *t*, and $CE_m^i(t)$ is the avoided $CO_2$ emissions from vehicle manufacturing for mode i (i = air, road and OSR) due to traffic diversion in the "with HSR" scenario relative to the "without HSR" scenario. The detailed calculation of $CE_m^H$, $CE_m^i$ and $NCE_m$ is provided in section 5.

Then, the net emissions derived from vehicle operation can be written as

$$NCE_o(t) = CE_o^H(t) - \sum_i CE_o^i(t) = E_h Q_h(t) - \sum_i E_i Q_i(t) \quad (7)$$

Where $CE_o^H(t)$ is the actual $CO_2$ emissions from operating HSR rolling stocks in year *t*, and $CE_o^i(t)$ is the avoided $CO_2$ emissions from vehicle operation due to traffic diversion from another transportation mode *i* to HSR. Let $E_h$ be the $CO_2$ emissions rate of HSR, and $E_i$ be the $CO_2$ emissions rate of the other transportation mode *i*. Then, using equation (2), we can convert equation (7) to

$$NCE_o(t) = E_h Q_G(t) - \sum_i (E_i - E_h) Q_i(t) \quad (8)$$

The first term of equation (8) indicates the extra emissions from operating HSR to accommodate generated traffic volume, comparing with the "without HSR" scenario. The second term of equation (8) represents the emissions reduction as some traffic volume is diverted from other modes to HSR. As HSR emits less than air and road but it emits more than OSR, traffic diversion from road and air will reduce $CO_2$ emissions, while traffic diversion from OSR will increase $CO_2$ emissions. Thus, the second term can be positive or negative depending on the traffic diverted from individual modes. The detailed calculation of each mode's emissions rate and the resulting $NCE_o$ is provided in Section 6.

The net emissions throughout the life cycle of the HSR infrastructure are the sum of $NCE(t)$ across all the time *t* from the completion of the construction to the end of the lifespan. That is, at the end of the lifespan of the infrastructure, the life-cycle net $CO_2$ emissions, denoted as $LNCE$, can be written as

$$LNCE = \sum_{t}^{lifetime}\{NCE_c(t) + NCE_m(t) + NCE_o(t)\} \tag{9}$$

Section 7 presents the calculation of LNCE. The lifespan of each transportation mode in concern is listed in Table 7.

Table 7 Modeled lifespans of infrastructures and vehicles of various transportation modes

| Transportation mode | Description | Lifespan |
|---|---|---|
| HSR & OSR | | |
| Civil engineering work | Subgrades, bridges & viaducts, tunnels, Station buildings | 100 years |
| Track | Rails | 30 years |
| Equipment | Telecom & signal equipment, energy provision equipment | 50 years |
| Rolling stocks | High Speed train CRH380, train 25G | 30 years |
| Expressway | | |
| Civil engineering work | Subgrades, bridges & viaducts, tunnels, Service Station buildings | 100 years |
| Pavement | Pavements | 30 years |
| Passenger cars | Cars (Buick GL8) | 10 years |
| Airport | | |
| Civil engineering work | Terminal building | 100 years |
| Runway | Runway | 30 years |
| Airplane | Airbus 320 | 20 years |

Source: Baron et al. (2011)

## 4. Net $CO_2$ Emissions from Infrastructure Construction ($NCE_c$)

The infrastructure of an HSR consists of subgrade, bridges and viaducts, tunnels, rails, railway equipment and stations. The main line of the B-S HSR is 1318 km long and it consists of 1061 km of bridges and viaducts, accounting for 80.4% of the total length, and 16 km of tunnels, accounting for 1.2% of the total length. There are 24 stations in the whole line. The emissions factors associated with constructing each unit of the infrastructure component of the B-S HSR are listed in Table 8. They are derived from the life-cycle inventory (LCI) of the HSR infrastructure construction included in the Carbon Footprint of the HSR Report (Baron et al., 2011). Applying these emissions factors, we obtain that bridges and viaducts account for 70% of the total $CO_2$ emissions from infrastructure construction, followed by rails 22.6%, subgrade 2.9%, railway equipment 2.5%, tunnels 1.5% and stations 0.6%.

According to Table 8, the construction of B-S HSR infrastructure generates 184,541 t CO2 per year during its entire lifetime, or 140 t CO2 per km yearly. This number lies on the upper end of the range provided by Baron et al. (2011), i.e. 58 to 176 t CO2 per km yearly. The construction of non-ballast track adopted by B-S HSR generates higher carbon footprint than the construction of ballast track. This is because many parts of China are covered by soft soils and hence viaducts are more commonly used than subgrade at ground level, which increases the CO2 emissions from construction work substantially (Wu et al., 2014).

Table 8 Carbon footprint of infrastructure construction of B-S HSR

| Components | Emissions factors [a] | Quantity [b] | CO2 emissions (t CO2 per year) | Share of CO2 emissions |
|---|---|---|---|---|
| Railway equipment | 3.5 t CO2 per km and year | 1318 km | 4613 | 2.5% |
| Rails | 31.6 t CO2 per km and year | 1318 km | 41649 | 22.6% |
| Subgrade | 22 t CO2 per km and year | 241 km | 5302 | 2.9% |
| Tunnels | 171 t CO2 per km and year | 16 km | 2736 | 1.5% |
| Viaducts | 115 t CO2 per km and year | 956 km | 109940 | 59.6% |
| Bridges | 183 t CO2 per km and year | 105 km | 19215 | 10.4% |
| Main Stations | 82 t CO2 per station and year | 6 stations | 492 | 0.3% |
| Secondary Stations | 33 t CO2 per station and year | 18 stations | 594 | 0.3% |
| Total | 140 t CO2 per km and year | 1318 km | 184541 | 100.0% |

Sources: [a] Baron et al. (2011), [b] Prospectus of Beijing-Shanghai HSR Co., Ltd

It is difficult to accurately calculate the CO2 emissions from infrastructure construction of the 1463 km B-S OSR, as this line was opened in 1933 and has gone through many new construction and expansion. Therefore, we apply the emissions factors of the 2315 km Beijing-Kowloon OSR. The Beijing-Kowloon OSR was built after 1990 and is in general consistent with the technical standards of the B-S OSR. According to Ren (2013), the construction of the Beijing-Kowloon OSR generated 114599 t CO2 per year, leading to an emissions factor of 49.5 t CO2 per km yearly. Based on this emissions factor, we estimate that the emissions from the construction of B-S OSR are 72,419 t CO2 per year.

The construction of the 1262 km B-S expressway lasted 13 years from 1987 to 2000. The majority of the B-S expressway has four lanes, but it has six lanes for about 155 km. We apply emissions factors from various sources and find that pavement accounts for 44.1% of CO2 emissions from the construction work of this expressway, subgrades 27.1%, bridges / viaducts 23.7%, tunnels 5.0% and service stations 0.1% (Table 9). The carbon footprint is estimated to be 97,365 t CO2 per year for the construction of the B-S expressway or 77 t CO2 per km yearly, which is close to the emissions of the B-S OSR.

Table 9 Annualized carbon footprint of infrastructure construction of B-S expressway

| Components | Emissions factor | Quantity | CO2 emissions | Share of CO2 |
|---|---|---|---|---|

| | | | (t CO2 per year) | emissions |
|---|---|---|---|---|
| Pavement | 34 t CO2 per km and year [a] | 1262 km | 42908 | 44.1% |
| Subgrade | 22 t CO2 per km and year [a] | 1201 km | 26422 | 27.1% |
| Tunnel | 375 t CO2 per km and year [b] | 13 km | 4875 | 5.0% |
| Bridges / viaducts | 481 t CO2 per km and year [b] | 48 km | 23088 | 23.7% |
| Service station | 3 t CO2 per station and year [c] | 24 stations | 72 | 0.1% |
| Total | 77 t CO2 per km and year | 1262 km | 97365 | 100.0% |

Sources: [a] Liu (2015), [b] Wang et al. (2014), [c] Yu et al. (2017)

Most airports in cities along the B-S corridor started operation in the 1990s. The only exceptions are Beijing Capital International Airport (PEK), Tianjin Binhai International Airport (TSN) and Shanghai Hongqiao International Airport (SHA), which started operation in 1950s. All the airports have been expanded as passenger traffic grows. Airport infrastructure mainly includes runways and terminals. The total carbon footprint for the construction of nine airports is 12,624 t CO2 per year, which is much lower than the B-S OSR and expressway.

Table 10 Annualized carbon footprint of infrastructure construction at airports

| Airport | Runway area (ha) | Runway emissions factor (t CO2 per ha and year) | Terminal area (ha) | Terminal emissions factor (t CO2 per ha and year) | CO2 emissions (t CO2 per year) |
|---|---|---|---|---|---|
| PEK | 61.6 | 18.2 [a] | 141.0 | 17.0 [b] | 3518 |
| TSN | 37.6 | | 36.4 | | 1303 |
| PVG | 86.6 | | 82.4 | | 2977 |
| SHA | 33.5 | | 51.0 | | 1477 |
| NKG | 43.2 | | 42.5 | | 1509 |
| TNA | 21.6 | | 11.4 | | 587 |
| XUZ | 17.0 | | 5.8 | | 408 |
| CZX | 17.0 | | 3.8 | | 374 |
| WUX | 16.0 | | 10.6 | | 471 |
| Total | 334.1 | | 384.9 | | 12624 |

Sources: [a] Yang and Al-Qadi (2017), [b] Cheng et al. (2020)

After obtaining the CO2 emissions from infrastructure construction of the four transportation modes, we calculate the CO2 emissions of infrastructure construction shared by each unit of traffic in Table 11. The maximum passenger traffic volume up to 2017 of the four transportation modes is calculated based on data provided in Appendix A. The proportion of passenger traffic over total traffic and the average trip distance are obtained from various sources listed under Table 11. It can be seen that HSR generates the highest construction-related emissions per unit of traffic, followed by highway, OSR and aviation.

Table 11 Comparison of annualized CO2 emissions from infrastructure constructions

| | B-S HSR | B-S OSR | B-S expressway | Air |
|---|---|---|---|---|
| CO2 emissions from construction (t CO2 per year) | 184541 | 72420 | 97365 | 12624 |
| Maximum annual passenger traffic up to 2017 (million persons) | 130.82 | 145.27 | 364.46 | 142.95 |

| | | | | |
|---|---|---|---|---|
| Average trip distance (km) | 637 | 535 | 100 | 1725 |
| Average share of passenger traffic over total traffic (passenger + freight) | 100% | 62% | 69% | 95% |
| $CO_2$ emissions of construction per unit of traffic (g $CO_2$ / p-km-year) | 2.21 | 0.58 | 1.84 | 0.05 |

Sources: Prospectus of Beijing-Shanghai HSR Co., Ltd; "Statistical analysis report of China's expressway traffic volume survey"(2011-2017); "Statistical data on civil aviation of China" (2011-2017)

After the entry of HSR, the other modes of transport may avoid some capacity expansion as part of the traffic is diverted to HSR relative to the "without HSR" scenario. We estimate the avoided infrastructure expansion due to the presence of HSR in the following way. Given that avoided infrastructure expansion occurs in non-HSR mode *i* (*i* = air, road and expressway), we use these modes' traffic difference between the "without HSR" scenario and the "with HSR" scenario to approximate the capacity avoided in the "with HSR" scenario relative to the "without HSR" scenario. In detail, for each mode $i \neq h$, as the amount of passenger traffic handled in the "without HSR" scenario in 2017, $Q_{i0}(2017)$, is expected to be larger than the maximum passenger traffic handled in the "with HSR" scenario up to the last year of data observation (i.e. 2017), $\max_t Q_{i1}(t)$, we consider the capacity avoided in the "with HSR" scenario as $\Delta Q_i = Q_{i0}(2017) - \max_t Q_{i1}(t)$. Then, we estimate the infrastructure capacity in the "with HSR" scenario ($K_{i1}$) with the following equation: $K_{i1} = \max_t Q_{i1}(t)/r_{i1}$, where $r_{i1}$ is the average share of passenger traffic over total traffic (the sum of passenger and freight traffic). Next, we represent the avoided capacity in terms of a proportion of infrastructure capacity in the "with HSR" scenario, i.e. $\rho_i = \Delta Q_i/K_{i1}$. Then, the annualized reduced $CO_2$ emissions due to avoided infrastructure expansion is calculated as the multiplication of mode *i*'s annualized $CO_2$ emissions from infrastructure construction and $\rho_i$ (Table 12).

Table 12 Annualized $CO_2$ emissions reduction due to avoided infrastructure expansion ($CE_c^i$)

| | B-S OSR | B-S expressway | Air |
|---|---|---|---|
| $CO_2$ emissions of construction (t $CO_2$ per year) | 72419 | 97365 | 12624 |
| Projected 2017 passenger traffic "without HSR" ($\boldsymbol{Q_{i0}(2017)}$, million persons) | 163.72 | 466.70 | 153.57 |
| Maximum passenger traffic up to 2017 "with HSR" ($\boldsymbol{\max_t Q_{i1}(t)}$, million persons) | 145.27 | 364.46 | 142.95 |
| Avoided capacity ($\boldsymbol{\Delta Q_i}$, million persons) | 18.45 | 102.24 | 10.62 |
| Average share of passenger traffic over total traffic ($\boldsymbol{r_{i1}}$) | 62% | 69% | 95% |
| Infrastructure capacity "with HSR" ($\boldsymbol{K_{i1}}$, million persons) | 234.31 | 528.20 | 150.47 |
| Proportion of infrastructure avoided ($\boldsymbol{\rho_i}$) | 8% | 19% | 7% |
| $CO_2$ emissions reduction due to avoided infrastructure expansion (t $CO_2$ per year) | 5793.52 | 18499.35 | 883.68 |

Based on equation (5) and all the information above, the annualized net $CO_2$ emissions from infrastructure construction is obtained below:

$$NCE_c(t) = CE_c^h(t) - \sum_i CE_c^i(t)$$
$$= 184{,}541 - 5{,}793.52 - 18{,}499.35 - 883.68$$
$$= 159{,}364.45 \ (\text{t CO2 per year})$$

Since the freight traffic of the B-S OSR has not increased as expected and the capacity has not been fully utilized, the avoided expansion due to HSR is not large. The avoided highway expansion can offset a large share of emissions from HSR construction, while the expansion of aviation infrastructure is negligibly small. As a result, the net CO2 emissions from the construction of the B-S HSR are still huge due to the small amount of avoided expansion of the other transportation modes.

## 5. Net CO2 Emissions from Vehicle Manufacturing ($NCE_m$)

We first estimate the number of train sets required under the design capacity of the B-S HSR. As shown in Table 13, the trains are in operation 18 hours or 1080 minutes per day (between 6 a.m. and 12 p.m.) and 30 minutes are taken for preparing and cleaning before each new ride. The number of journeys per day and train is the ratio of the operation time and the total time for travel and preparation. The number of needed trains for operation is the ratio of the total number of trains per day and the number of journeys per day and train. It is assumed that 80% of the trains are in service while 20% are in stock for cleaning, maintenance and repair. Since the design capacity of the B-S HSR is 160 pairs of trains per day, a total of 134 trains are needed.

Table 13 Estimation on the number of trains for the B-S HSR

| | | |
|---|---|---|
| Operation time per day | [min] | 1080 |
| Number of trains per day and direction | [Nr] | 160 |
| Total number of trains per day | [Nr] | 320 |
| Travel time | [min] | 300 |
| Total time for travel incl. preparation | [min] | 330 |
| Number of journeys per day and train | [Nr] | 3 |
| Needed trains for operation | [Nr] | 107 |
| Reserve stock (maintenance & repairing) | [Nr] | 27 |
| Grand sum | [Nr] | 134 |

The most commonly used train model on the B-S HSR is CRH380BL marshalling 16 units. The emissions from the manufacturing of this train model are estimated to be 13000 t CO2, since the emissions from the production of CRH380B marshalling 8 units are 6500 t CO2 (Baron et al., 2011). Then, the total carbon footprint for manufacturing HSR rolling stocks is estimated to be 58067 t CO2 per year, which can be converted to 0.29 g CO2 / p-km according to the 2017 HSR traffic (Table 14).

Table 14 Annualized CO2 emissions from the manufacturing of HSR rolling stocks

| | | |
|---|---|---|
| Number of trains | [Nr] | 134 |
| The manufacturing emissions per train (t CO2) | [t CO2] | 13000 |
| Total emissions for rolling stock | [t CO2] | 1742000 |
| Total emissions for rolling stock per year | [t CO2] | 58067 |
| Number of seats per vehicle | | 1318 |
| Load factor | | 0.75 |
| Average mileage per year | [km] | 1533000 |
| Emissions for rolling stock manufacturing per unit of traffic | [g CO2/p-km-year] | 0.29 |

Table 15 presents the calculation of avoided vehicles to be manufactured and the corresponding emissions from manufacturing these vehicles. On the B-S OSR line, EMU G25 is commonly used with 1376 seats and an average load factor of about 80%. Assuming that the EMU can operate for 12 hours per day and the speed is 100 km/h, the annual operating distance is 438000 km. According to Statistical Analysis Report of China's Expressway Traffic Volume Survey, the number of seats of an average passenger vehicle is 6.43 and the average load factor is 48%. Therefore, the average number of passengers per vehicle on the expressways is 3.08 in China. Based on these national-level figures, we chose Buick GL8 to calculate CO2 emissions from passenger vehicle manufacturing as this vehicle model has 7 seats and a load factor of 44%. According to China's regulation, passenger cars that have run more than 600,000 km are recommended to be scrapped. Assuming a 10-year life cycle of a passenger car, the maximum travel distance of a passenger car is 60,000 km per year. In terms of air transport, Airbus A320 is commonly used on routes between Beijing and Shanghai which has 150 seats and an average load factor of about 65%. Assuming a 20-year life cycle, the maximum flight time is about 3000 hours per year, and the annual flight distance is 2400000 km, assuming an average speed of 800 km/h.

Table 15 Annualized CO2 emissions reduction due to avoided vehicle manufacturing ($CE_m^i$)

| | B-S OSR | B-S Expressway | B-S Air |
|---|---|---|---|
| Diverted passenger traffic in 2017 (million p-km) | 7663 | 12170 | 1077 |
| Vehicle model | EMU G25 | Buick GL8 | Airbus A320 |
| Number of seats per vehicle | 1376 | 7 | 150 |
| Load factor | 0.8 | 0.44 | 0.65 |
| Average operating distance per year (km) | 438000 | 60000 | 2400000 |
| Number of vehicles avoided | 16 trains | 65855 cars | 5 airplanes |
| Emissions of vehicle construction, maintenance and disposal (t CO2 per vehicle) [a] | 13000 | 7.2 | 2258 |
| Emissions for vehicle manufacturing per unit of traffic (g CO2/p-km-year) | 0.90 | 3.90 | 0.48 |

| | | | |
|---|---|---|---|
| Total emissions of avoided vehicle manufacturing (t CO2) | 206614 | 474156 | 10393 |
| Emissions of avoided vehicle manufacturing per year (t CO2) | 6887 | 47416 | 520 |

Sources: Baron et al. (2011)

Then, using the diverted passenger traffic of the B-S HSR in 2017, we can calculate the number of extra OSR trains, passenger cars and airplanes required to accommodate the diverted traffic in the "without HSR" scenario. That is, these vehicles will not be produced in the "with HSR" scenario. Then, the CO2 emissions from avoided manufacturing vehicles are the multiplication of the emissions from manufacturing per vehicle and the number of avoided vehicles. Tables 14 and 15 also present the CO2 emissions from vehicle manufacturing per unit of traffic, which is the highest for cars, followed by OSR trains, airplanes and HSR trains. This is because passenger cars have fewer seats, lower load factor, lower frequency of use and shorter life cycle than the other transportation modes.

The annualized net CO2 emissions from vehicle manufacturing can be calculated with equation (6).

$$NCE_m(t) = CE_m^h(t) - \sum_i CE_m^i(t)$$
$$= 58067 - 6887 - 47416 - 520$$
$$= 3254 \ \ (\text{t CO2 per year})$$

We can see that majority of the emissions from the manufacturing of HSR rolling stocks is offset by the avoided emissions as fewer passenger vehicles are produced due to traffic diversion from the B-S expressway, leading to a small $NCE_m$.

## 6. Net CO2 Emissions from Vehicle Operation ($NCE_o$)

6.1 CO2 emissions rate of HSR operation

HSR trains rely on electric power and essentially do not generate CO2 during operation. However, electric energy for railway operation in China mainly comes from thermal power generation, and a large amount of CO2 is produced in the process of coal-fired power generation. Thus, to calculate the CO2 emissions per unit of traffic (CO2 emissions rate) due to operating the B-S HSR trains, we first calculate the power consumption per unit of traffic, and then multiply it with the CO2 emissions coefficient of one unit of electric power in the region. That is,

$$E_h = EC_h \times C_e \tag{10}$$

where $EC_h$ represents energy consumption per p-km of HSR, and $C_e$ represents the CO2 emissions coefficient of electric power. The B-S HSR only operated for six months in 2011. Since 2012, the energy consumption per gross ton-km has become stable, which is about 0.039 KWH per ton-km (Table 16). With the increase in ridership and hence load factor, the energy consumption per p-km gradually decreased from 2012 to 2017, indicating the existence of strong economies of scale.

Table 16 Energy consumption per unit of traffic for operating B-S HSR

| Year | 2011 | 2012 | 2013 | 2014 | 2015 | 2016 | 2017 |
|---|---|---|---|---|---|---|---|
| KWH per gross ton-km | 0.024 | 0.039 | 0.039 | 0.039 | 0.039 | 0.039 | 0.039 |
| KWH per p-km ($EC_h$) | 0.042 | 0.049 | 0.042 | 0.036 | 0.033 | 0.033 | 0.029 |

Note: KWH stands for Kilowatt-hour
Source: Beijing-Shanghai HSR Co., Ltd

As shown in Table 17, the emissions coefficient of electric power in the B-S corridor decreased from 0.748 t CO2 per MWH in 2011 to 0.641 t CO2 per MWH in 2017, which reflects the decreasing share of thermal power generation in China and the technology advancement in thermal power generation. Therefore, the CO2 emissions rate of B-S HSR has been quickly reduced. In 2017, the emissions rate was 18.85 t CO2 per million p-km, nearly half of that in 2012. With the development of technology and the adjustment of energy structure, the CO2 emissions level of China's HSR will be further reduced in the future. On the other hand, with the increase in passenger ridership of the B-S HSR, the CO2 emissions rate will be further reduced.

Table 17 CO2 emissions rate of B-S HSR

| Year | 2011 | 2012 | 2013 | 2014 | 2015 | 2016 | 2017 |
|---|---|---|---|---|---|---|---|
| National share of thermal power over total power [a] | 82% | 79% | 78% | 76% | 74% | 73% | 72% |
| Emissions coefficient [a] ($C_e$) (t CO2 per MWH) | 0.748 | 0.725 | 0.722 | 0.714 | 0.690 | 0.664 | 0.641 |
| CO2 emissions rate ($E_h$) (t CO2 per million p-km) | 31.10 | 35.68 | 30.24 | 25.42 | 22.88 | 21.85 | 18.85 |

Note: MWH stands for million watt-hour
Source: [a] 2011-2017 Baseline Emissions Factors for Regional Power Grids in China.

## 6.2 CO2 emissions rate of OSR operation

Similar to Section 6.1, the CO2 emissions rate of the B-S OSR can be obtained by equation (11).

$$E_3 = EC_3 \times C_e \tag{11}$$

where $EC_3$ represents energy consumption per unit of traffic of OSR. Since the B-S OSR belongs to three different railway companies, data about the energy consumption of this line is not available. Referring to the results of a survey conducted in 2010, the unit energy consumption of the Wuhan-Guangzhou OSR is 0.016 KWH per gross ton-km and 0.016 KWH per p-km (Wu, 2014). Since the locomotive traction technology and train dispatching method adopted by the B-S OSR and Wuhan-Guangzhou OSR are very similar, it is assumed that the energy consumption per gross ton-km is the same. Since the passenger volume of the B-S OSR did not changed much from 2011 to 2017 (Table 3), it is assumed that the energy consumption per p-km is the same across years. Applying the same CO2 emissions coefficients provided in Table 17, the CO2 emissions rate of B-S OSR can be obtained (Table 18).

Table 18 Energy consumption and CO2 emissions rate of B-S OSR

| Year | 2011 | 2012 | 2013 | 2014 | 2015 | 2016 | 2017 |
|---|---|---|---|---|---|---|---|
| KWH per gross ton km [a] | 0.016 | 0.016 | 0.016 | 0.016 | 0.016 | 0.016 | 0.016 |
| KWH per p-km [a] ($\boldsymbol{EC_3}$) | 0.016 | 0.016 | 0.016 | 0.016 | 0.016 | 0.016 | 0.016 |
| CO2 emissions rate ($\boldsymbol{E_3}$) (t CO2 per million p-km) | 12.19 | 11.82 | 11.77 | 11.64 | 11.25 | 10.82 | 10.45 |

Source: [a] Wu (2014).

It can be seen that HSR consumes more energy per unit of traffic than OSR due to higher speed. According to our estimation, the energy consumption and CO2 emissions rate of the B-S HSR is almost twice of the B-S OSR in 2017 if the capacity of OSR is fully utilized. Otherwise, the difference will be even larger.

### 6.3 CO2 emissions rate of road vehicle operation

The passenger traffic of the B-S expressway comes from buses and private vehicles. Similar to Sections 6.1 and 6.2, the CO2 emissions rate of passenger cars is defined in equation (12).

$$E_1 = EC_1 \times C_g \tag{12}$$

where $EC_1$ represents the energy consumption per unit of passenger traffic averaged across buses and cars, and $C_g$ is the CO2 emissions coefficient of standard gasoline consumption (3.04 kg CO2/kg). $EC_1$ can be calculated by

$$EC_1 = r \times EC_b + (1 - r)EC_v \tag{13}$$

where $EC_b$ represents energy consumption per unit of bus traffic, $EC_v$ is energy consumption per unit of private vehicle, and $r$ is the share of bus traffic over total road passenger traffic which is estimated to be 9%.

National statistical data on energy consumption of buses is available in China, which is used to approximate energy consumption of buses per unit of traffic on the B-S expressway.

However, data on energy consumption of private passenger vehicles is not available and needs to be estimated with equation (14).

$$EC_v = \frac{\sum_{i=1}^{3} TV_i \times FC_i}{\sum_{i=1}^{3} TV_i \times SC_i \times LF_i} \tag{14}$$

where $TV_i$ is the traffic share of each vehicle type $i$ on the Jiangsu section of the B-S expressway, $FC_i$ is the amount of fuel consumption, $SC_i$ is the seating capacity, and $LF_i$ stands for load factor. Three types of passenger vehicles are considered, small, medium, and large, and their definitions are provided in Table 19.

Table 19 Classification of passenger vehicles and fuel consumption

| Types | Seating capacity | Gasoline consumption (L/100km) |
|---|---|---|
| Small | ≤ 9 | 8.80 |
| Medium | 10-19 | 21.14 |
| Large | ≥ 20 | 23.11 |

Source: "Statistical analysis report of China's expressway traffic volume survey"

As shown in Table 20, the energy consumption per unit of bus traffic increased slightly from 2011 to 2017, probably due to the reduced traffic congestion and improved comfort. The energy consumption per unit of private car traffic had little change during the 2011-2017 period. On the per unit of traffic basis, buses only consume 1/3 to 1/2 of the energy consumed by private vehicles. However, bus traffic only accounts for a small share of highway passenger traffic, and as a result the $CO_2$ emissions rate of highway vehicles is much higher than that of HSR.

Table 20 Energy consumption and $CO_2$ emissions rate of road vehicles

| Year | | 2011 | 2012 | 2013 | 2014 | 2015 | 2016 | 2017 |
|---|---|---|---|---|---|---|---|---|
| Tons of standard gasoline[5] per million p-km | Operating buses [a] ($EC_b$) | 7.91 | 8.19 | 8.12 | 8.47 | 8.82 | 10.15 | 10.29 |
| | Private vehicles [b] ($EC_v$) | 23.94 | 24.01 | 23.73 | 23.80 | 23.87 | 23.94 | 23.94 |
| | Average ($EC_1$) | 22.47 | 22.54 | 22.33 | 22.40 | 22.47 | 22.68 | 22.61 |
| Ton CO2 per million p-km (**$E_1$**) | | 68.31 | 68.52 | 67.88 | 68.09 | 68.31 | 68.95 | 68.73 |

Source: [a] 2011-2017 Statistical bulletin on the development of transportation industry in China. [b] Statistical Analysis Report of China's Expressway Traffic Volume Survey (2011-2017)

### 6.4 $CO_2$ emissions rate of aircraft operation

The $CO_2$ emissions rate of passenger airplane can be expressed as:

$$E_2 = EC_2 \times C_k \tag{15}$$

Where $EC_2$ represents the energy consumption per unit of air passenger traffic, and $C_k$ is the

[5] 1kg standard Gasoline = 10000 kcal

CO2 emissions coefficient of aviation kerosene consumption (3.15 kg CO2/kg)[6]. $EC_2$ can be obtained by equation (16):

$$EC_2 = \frac{\sum \delta \times S \times V}{\sum H} \quad (16)$$

Where $\delta$ represents aviation fuel consumption per seat-km, $S$ is the number of seats available for each flight segment, $V$ is the distance of each segment, and $H$ is the passenger turnover of each section. The traffic data of the main air segments, i.e. Beijing-Shanghai, Tianjin-Shanghai and Nanjing-Beijing, are shown in Appendix B. The fuel consumption data of different flight ranges are published by European Environment Agency - EEA. Aircraft consume much more fuel in the take-off and landing stages, when the aircraft needs to climb and descend rapidly, than in the cruise stage. As shown in Table 21, the fuel consumption of a flight segment shorter than 250 km is 75.7 g / seat-km, while that of flights over 1000 km is only 19 g / seat-km.

Table 21 Aviation fuel consumption by range class

| Range class (km) | Aviation kerosene consumption (g / seat-km) |
|---|---|
| 125 | 120.5 |
| 250 | 75.7 |
| 375 | 60.1 |
| 500 | 42.7 |
| 625 | 38.4 |
| 750 | 36.0 |
| 1000 | 33.2 |
| >1000 | 19.0 |

Source: EMEP/EEA air pollutant emission inventory guidebook 2019

According to Table 22, the three air routes in the B-S corridor are improving their fuel efficiency continuously, as the energy consumption and CO2 emissions rate have decreased from 2011 to 2017.

Table 22 Energy consumption and CO2 emissions rate of aircraft operation

| Year | 2011 | 2012 | 2013 | 2014 | 2015 | 2016 | 2017 |
|---|---|---|---|---|---|---|---|
| Tons of aviation kerosene per million p-km ($EC_2$) | 30.73 | 30.03 | 27.65 | 27.65 | 26.76 | 26.63 | 26.50 |
| CO2 emissions rate ($E_2$) (t CO2 per million p-km) | 96.80 | 94.60 | 87.10 | 87.10 | 84.30 | 83.90 | 83.48 |

From Sections 6.1-6.4, we can conclude that air transport has the highest CO2 emissions rate during vehicle operation, followed by road, HSR and OSR (Figure 3). Taking 2017 as an

[6] Data source: Civil aviation comprehensive statistical survey system 2018.

example, the $CO_2$ emissions rate of air is 4.4 times of HSR, that of road is 3.6 times of HSR, and that of HSR is 1.8 times of OSR.

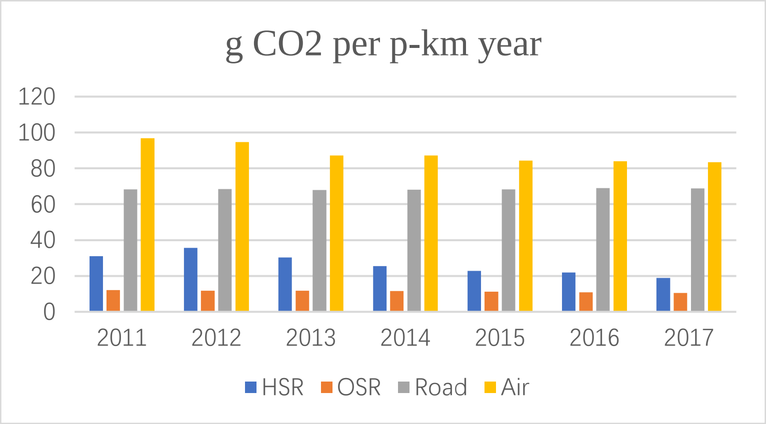


Figure 3. $CO_2$ emissions per unit passenger traffic of 4 modes in B-S corridor

6.5 Calculation of net $CO_2$ emissions from vehicle operation

According to equation (8), the calculation of net $CO_2$ emissions from vehicle operation requires the information about $CO_2$ emissions rate as well as diverted and generated traffic volume in each section from 2011 to 2017. As the latter is provided in Appendix A in the form of passenger numbers, we need to convert diverted and generated traffic into the form of traffic turnover, i.e. p-km, by multiplying the passenger number with the distance of each section. Base on the above data, $CO_2$ emissions in each section from 2011 to 2017 are calculated with equation (8) and the details are provided in Appendix C. The annual net $CO_2$ emissions from vehicle operation are shown in Table 23. It can be found that $CO_2$ emissions from diverted traffic have been increasing for the first three years. This is because in the initial stage, the diverted traffic of HSR mainly comes from OSR, with 62.27% in 2011, 54.9% in 2012 and 44.99% in 2013, while the diverted traffic from road increases later than OSR, with 31.80% in 2011, 30.32% in 2013 and 50.16% in 2017 and the diverted traffic from aviation has a similar pattern, with 2.08% in 2011, 4.23% in 2013 and 4.44% in 2017. At the same time, the $CO_2$ emissions rate of HSR is greatly reduced as its ridership increases, but that of the other ground modes has almost no change because highway has little scale economy and OSR has little change in traffic volume. Although $CO_2$ emissions rate of civil aviation is slightly reduced, its share of diverted traffic volume is very small. These two forces together cause the $CO_2$ emissions of diverted traffic to become negative in 2014 with an increasing magnitude over time.

Table 23 Net $CO_2$ emissions from vehicle operation ($NCE_o$): 2011-2017

| Year | Emissions from diverted traffic (t CO2) | Emissions from generated traffic (t CO2) | Total (t CO2) |
|---|---|---|---|
| 2011 | 68272.49 | 113496.34 | 181768.83 |
| 2012 | 261762.07 | 253536.01 | 515298.08 |
| 2013 | 41397.88 | 376330.75 | 417728.63 |
| 2014 | -336164.52 | 519281.03 | 183116.51 |
| 2015 | -376031.03 | 425507.60 | 49476.57 |
| 2016 | -558188.87 | 422263.70 | -135925.16 |
| 2017 | -771169.50 | 483243.50 | -287926.00 |

The CO2 emissions of the generated traffic are positive because people generate higher travel demand under the "with HSR" scenario than the "without HSR" scenario. Furthermore, the net CO2 emissions from vehicle operation has become negative since 2016, which indicates that although more travel demand is accommodated with HSR, the CO2 emissions from vehicle operation in the B-S corridor are still lower than the case without HSR.

## 7. Lifetime Net CO2 Emissions ($LNCE$)

The lifetime net CO2 emissions, $LNCE$ can be obtained with equation (9). The result is presented in Table 24. As the net emissions from infrastructure construction are 159,364.45 t CO2 per year, the lifetime value is 15,936,445 t CO2. Assuming that the infrastructure is constructed before the project operation, CO2 emissions from infrastructure construction need to be compensated by the emissions reduction during the operation period. The net emissions from vehicle manufacturing are 3254 t CO2 per year, which is calculated based on the 2017 observed traffic data. Since we only have actual traffic data up to 2017, we need to make assumptions for the net emissions after 2017. It is assumed that vehicles are always equipped according to the design capacity during the operation, and thus the net CO2 emissions from vehicle manufacturing are consistent every year. Regarding the net emissions from vehicle operation after 2017, we apply the following approach. According to the experience of Shinkansen in Japan, TGV in France and other HSRs, the traffic volume of a new HSR project will grow in the initial stage of operation, and then it will enter a stable stage in about 10 years. We fit a linear model by regressing the net emissions from vehicle operation on the time variable for the 2012 – 2017 periods (Note that B-S HSR only operated for half a year in 2011).[7] Then, we project the net emissions in the 2018-2021 periods with the linear model,[8] and assume that the net emissions from vehicle operation remain unchanged after 2021.

[7] The goodness-of-fit (R-squared) is 0.99.
[8] The calculation does not take into account the impact of COVID-19.

Table 24 Lifetime net $CO_2$ emissions of the B-S HSR project

| Lifetime (year) | Net emissions from infrastructure construction (t $CO_2$) | Net emissions from vehicle manufacturing (t $CO_2$) | Net emissions from vehicle operation (t $CO_2$) |
|---|---|---|---|
| 0 | 15936445 | | |
| 1 (2011) | | 3254 | 181769 |
| 2 (2012) | | 3254 | 515298 |
| 3 (2013) | | 3254 | 417729 |
| 4 (2014) | | 3254 | 183117 |
| 5 (2015) | | 3254 | 49477 |
| 6 (2016) | | 3254 | -135925 |
| 7 (2017) | | 3254 | -287926 |
| 8 (2018) | | 3254 | -457447 |
| 9 (2019) | | 3254 | -623468 |
| 10 (2020) | | 3254 | -789489 |
| 11 (2021) | | 3254 | -955510 |
| 12 (2022) | | 3254 | -955510 |
| ⋮ | | ⋮ | ⋮ |
| 100 (2110) | | 3254 | -955510 |

Based on the information presented in Table 24, it is straightforward to find that the lifetime net $CO_2$ emissions of the B-S HSR project will be negative after the 26th year of operation. That is, the increased $CO_2$ emissions from infrastructure construction and vehicle manufacturing can be completely offset by the emissions reduction from vehicle operation within 26 years. Baron et al. (2011) estimated that the net $CO_2$ emissions of “LGV Mediterranée” HSR project will become positive after 5.3 years of operation, but we find a much longer payback period for the B-S HSR. There are two reasons. First, since a large proportion of HSR traffic is diverted from OSR and HSR has higher $CO_2$ emissions rate of train operation than OSR, the mode substitution effect of HSR causes an increase in net $CO_2$ emissions from vehicle operation in the earlier stage. Second, buses, which tend to emit less than private cars, are considered when calculating highway $CO_2$ emissions. This treatment lowers the average emissions rate of vehicle operated on expressways and reduces the effectiveness of emissions reduction via road traffic diversion.

The project can only achieve such a good effect with high HSR traffic density and sufficient traffic diversion from road and air. The emissions reduction effect of the B-S HSR project mainly comes from the vehicle operation stage. In the initial stage of operation, the diverted traffic is mainly from OSR, which can not reduce $CO_2$ emissions. As the traffic density on the HSR line increases, the improvement of mobility gradually attracts more passengers from road and air, and these two parts of diverted traffic are the main causes of $CO_2$ emissions reduction. The construction of HSR infrastructure will produce huge $CO_2$ emissions.

In the context of continuously growing travel demand, this part of $CO_2$ emissions can be offset in part by the reduction of expansion projects of the other transportation modes. The manufacturing of HSR rolling stocks can also generate a large amount of $CO_2$ emissions. If the diverted road traffic is high, most of these $CO_2$ emissions can be offset by reduced demand for passenger vehicles.

## 8. Conclusion

In this paper, we assess the lifetime net $CO_2$ emissions of the B-S HSR project. As the entry of B-S HSR affects the traffic of other transportation modes, such as air, road and OSR, along the B-S corridor, we compare the $CO_2$ emissions of two scenarios, one with HSR and the other without HSR. We incorporate both the mode substitution effect and traffic generation effect of HSR in the assessment of $CO_2$ emissions. A simplified LCA is adopted. That is, the $CO_2$ emissions from infrastructure construction, vehicle manufacturing and vehicle operation are all calculated. The $CO_2$ emissions per unit of traffic in each stage and by each transportation mode are shown in Table 25.

Table 25 $CO_2$ emissions per unit of traffic in the B-S corridor

| | HSR | OSR | Expressway | Air |
|---|---|---|---|---|
| $CO_2$ emissions from construction (g $CO_2$/p-km-year) | 2.21 | 0.58 | 1.84 | 0.05 |
| $CO_2$ emissions from vehicle manufacturing (g $CO_2$/p-km-year) | 0.29 | 0.9 | 3.9 | 0.48 |
| $CO_2$ emissions from vehicle operation (g $CO_2$/p-km-year) | 18.85 | 10.45 | 68.73 | 83.48 |

$CO_2$ emissions from infrastructure construction are mainly generated before the operation of HSR. Some recent studies, such as Chang et al. (2019) and Cheng et al. (2020), estimated a higher level of $CO_2$ emissions from HSR infrastructure construction, because they include more items throughout the building material supply chain. HSR has higher $CO_2$ emissions from infrastructure construction than OSR, expressway and air. Although a large share of HSR traffic is diverted from the other transportation modes, the avoided infrastructure expansion of those other modes has little effect in offsetting the infrastructure construction emissions of HSR. Generally speaking, $CO_2$ emissions from the construction of a new HSR line are a huge burden.

HSR has lower $CO_2$ emissions from vehicle manufacturing than in the other stages. On the basis of per unit of traffic, HSR also has lower $CO_2$ emissions from vehicle manufacturing than the other transportation modes, especially the highway. Since a considerable amount of traffic is diverted from the highway, the $CO_2$ emissions from the manufacturing of rolling stocks can be largely offset. Therefore, the annual $CO_2$ emissions burden from vehicle manufacturing is very small.

The emissions reduction effect of an HSR project mainly comes from vehicle operation. The emissions rate of B-S HSR has continuously decreased as the traffic density of HSR increases over time. Overall, OSR has the lowest emissions rate, followed by HSR, road and then air. Since most of the diverted traffic came from OSR in the earlier stage, the $CO_2$ emissions of the diverted traffic were increased in the first three years. As road and air increased their share of diverted traffic to about 40%-50%, the $CO_2$ emissions of the diverted traffic eventually turned to negative in 2014, and the net $CO_2$ emissions from vehicle operation turned to negative two years later.

Finally, we find that newly generated $CO_2$ emissions due to HSR infrastructure construction and vehicle manufacturing can be completely offset by the reduction in $CO_2$ emissions from vehicle operation after 26 years of HSR operation. The B-S HSR project has improved the average travel speed and accommodated new travel demand in the B-S corridor. While bringing these benefits, the lifetime net $CO_2$ emissions of the corridor are lower than the scenario without the project. For other HSR projects with lower traffic volume, the $CO_2$ emissions payback period is expected to be longer.

This study examines the net $CO_2$ emissions in the transportation sector after the entry of HSR, because we take an engineering approach and focus mainly on the calculation of $CO_2$ emissions. That is, we ignore the impact of HSR on the entire economy, including the consumption and production of all types of goods and services. In the future, a more comprehensive assessment of the impact of HSR on the $CO_2$ emissions of the entire economy can be conducted via modeling the relationship between HSR and all other sectors with for example the CGE models. Another limitation of this paper is that only $CO_2$ emissions are included in the analysis while other non-$CO_2$ greenhouse gases are excluded. A future study may incorporate all the greenhouse gases in the assessment.

## Acknowledgements

This paper is supported by the research project of the National Social Science Fund of China, "Economic Evaluation System Restructuring for High-Speed Rail Projects" (Project number: 18BJY170).

## References

Akerman, J., 2011. The role of high-speed rail in mitigating climate change – The Swedish case Europabanan from a life cycle perspective. *Transportation Research Part D: Transport and Environment* 16: 208-217.

Avetisyan, M., 2018. Impacts of global carbon pricing on international trade, modal choice and emissions from international transport. *Energy Economics* 76(OCT.): 532-548.

Baron, T., Martinetti, G., and Pepion, D., 2011. Carbon footprint of high-speed rail. International Union of Railways (UIC), Paris.

Baumeister, S., 2019. Replacing short-haul flights with land-based transportation modes to reduce greenhouse gas emissions: The case of Finland. *Journal of Cleaner Production* 225: 262-269.

Bueno, G., Hoyos, D., and Capellan-Perez, I., 2017. Evaluating the environmental performance of the high-speed rail project in the Basque Country, Spain. *Research in Transportation Economics* 62: 44-56.

Chang, B., and Kendall, A., 2011. Life cycle greenhouse gas assessment of infrastructure construction for California's high-speed rail system. *Transportation Research Part D: Transport and Environment* 16: 429-434.

Chang, Y., Lei, S., Teng, J., Zhang, J., Zhang, L., and Xu, X., 2019. The energy use and environmental emissions of high-speed rail transportation in China: A bottom-up modeling. *Energy* 182: 1193-1201.

Cheng, Y.H., 2010. High-speed rail in Taiwan: New experience and issues for future development. *Transport Policy* 17: 51-63.

Cheng, S., Lin, J., Xu, W., Yang, D., Liu, J., and Li, H., 2020. Carbon, water, land and material footprints of China's high-speed railway construction. *Transportation Research Part D: Transport and Environment* 82, 102314. https://doi.org/10.1016/j.trd.2020.102314

Chester, M., and Horvath, A., 2010. Life-cycle assessment of high-speed rail: the case of California. *Environ. Res. Lett.* 5(1), 014003. http://dx.doi.org/10.1088/1748-9326/5/1/014003

Chester, M., and Horvath, A., 2012. High-speed rail with emerging automobiles and aircraft can reduce environmental impacts in California's future. *Environ. Res. Lett.* 7(3), 034012.

Chester, M.V., and Ryerson, M.S., 2014. Grand challenges for high-speed rail environmental assessment in the United States. *Transportation Research Part A: Policy and Practice* 61: 15-26.

Cristea, A., Hummels, D., Puzzello, L., and Avetisyan, M., 2013. Trade and the greenhouse gas emissions from international freight transport. *Journal of Environmental Economics and Management* 65(1): 153-173.

Dalkic, G., Balaban, O., Tuydes-Yaman, H., and Celikkol-Kocak, T., 2017. An assessment of the CO2 emissions reduction in high-speed rail lines: Two case studies from Turkey. *Journal of Cleaner Production* 165: 746-761.

De Rus, G., and Inglada, V., 1997. Cost-benefit analysis of the high-speed train in Spain. *The Annals of Regional Science* 31(2): 175-188.

Givoni, M., and Dobruszkes, F., 2013. A review of ex-post evidence for mode substitution and induced demand following the introduction of high-speed rail. *Transport Reviews* 33(6): 720-742.

Hagedom, T., and Sieg, G., (2019). Emissions and external environmental costs from the perspective of differing travel purposes. *Sustainability* 11(24): 7233.

Inglada, V., and Coto-Millan, P., 2003. Social benefits of investment projects: The case for high-speed rail. *Contributions to Economics* 1: 361-386.

Janic, M., 2003. High-speed rail and air passenger transport: A comparison of the operational environmental performance. *Proceedings of the Institution of Mechanical Engineers, Part F: Journal of Rail & Rapid Transit* 217: 259-269.

Kaewunruen, S., Sresakoolchai, J., and Peng, J., 2019. Life cycle cost, energy and carbon assessments of Beijing-Shanghai high-speed railway. *Sustainability* 12(1): 206.

Lawrence, M., Bullock, R., and Liu, Z, 2019. China's high-speed rail development. The World Bank, pp. 69-79. https://openknowledge.worldbank.org/handle/10986/31801.

Lee, J.-H., Chon, K.-S., and Park, C., 2004. Accommodating heterogeneity and heteroscedasticity in intercity travel mode choice model: Formulation and application to HoNam, South Korea, high-speed rail demand analysis. *Transportation Research Record* 1898(1): 69-78.

Li, H., Wang, K., Yu, K., and Zhang, A., 2020. Are conventional train passengers underserved after entry of high-speed rail? - Evidence from Chinese intercity markets, *Transport Policy* 95: 1-9.

Liu, S., 2015. Comparative study on the environmental impact of infrastructure construction of Beijing Shanghai Expressway and Beijing Shanghai high speed railway based on LCA. Master of Engineering, Southeast University, Nanjing, China. (in Chinese)

Liu, S., Wan, Y. and Zhang, A., 2020. Does China's high-speed rail development lead to regional disparities? A network perspective. *Transportation Research Part A: Policy and Practice* 138, 299-321.

Otsuka, A., 2020. Assessment of the improvement in energy intensity by the new high-speed railway in Japan. *Asia-Pacific Journal of Regional Science*, DOI: https://doi.org/10.1007/s41685-020-00165-5.

Ren, F., Guo, X., Liang, R., Liu, H., 2013. Life cycle carbon dioxide emissions assessment of railway construction. *Journal of Beijing Jiaotong University* 37(01): 115-119. (In Chinese)

Scott, K., 2011. How big are the environmental benefits of high-speed rail? A cost-benefit analysis of high-speed rail replacing automobile travel in the Georgetown-San Antonio corridor. Masters of Public Administration, Texas State University, San Marcos, TX.

Sims R., R. Schaeffer, F. Creutzig, X. Cruz-Núñez, M. D'Agosto, D. Dimitriu, M. J. Figueroa Meza, L. Fulton, S. Kobayashi, O. Lah, A. McKinnon, P. Newman, M. Ouyang, J. J. Schauer, D. Sperling, and G. Tiwari, 2014. Transport. In: Climate Change 2014: Mitigation of Climate Change. Contribution of Working Group III to the Fifth Assessment Report of the Intergovernmental Panel on Climate Change [Edenhofer, O., R. Pichs-Madruga, Y. Sokona, E. Farahani, S. Kadner, K. Seyboth, A. Adler, I. Baum, S. Brunner, P. Eickemeier, B. Kriemann, J. Savolainen, S. Schlömer, C. von Stechow, T. Zwickel and J.C. Minx (eds.)]. Cambridge University Press, Cambridge, United Kingdom and New York, NY, USA.

Sun, Y., Lin, Z., and Lin, X., 2018. Research on the important role of Beijing-Shanghai high-speed railway in economic and social development. Chinese Academy of Engineering, Beijing. (In Chinese)

Wang, K., Xia, W., Zhang, A., and Zhang, Q., 2018. Effects of train speed on airline demand and price: Theory and empirical evidence from a natural experiment. *Transportation Research Part B: Methodological* 114: 99-130.

Wang, X., Zhang, H., and Fu, Y., 2016. Study on calculation method of vehicle exhaust emissions. *Highway Transportation Technology* 32（01）: 130-133. (In Chinese)

Wang, X., Wu L., and Yang D., 2014. Expressway construction CO2 emissions calculation and analysis. *Highway Transportation Science and Technology* 31 (02): 150-158 (In Chinese)

Westin, J., and Kageson, P., 2012. Can high speed rail offset its embedded emissions? *Transportation Research Part D: Transport and Environment* 17: 1-7.

Wu, J., 2014. The financial and economic assessment of China's high-speed rail investments: A preliminary analysis. *The Economics of Investment in High-Speed Rail*, OECD Publishing, 129-162. http://dx.doi.org/10.1787/9789282107751-en.

Wu, J., Nash, C., and Wang, D., 2014. Is high speed rail an appropriate solution to China's rail capacity problems? *Journal of Transport Geography* 40: 100-111.

Yang, R., and Al-Qadi, I.L., 2017. Development of a life-cycle assessment tool to quantify the environmental impacts of airport pavement construction. *Transportation Research Record: Journal of the Transportation Research Board* 2603: 89-97.

Yu, K., Cheng, D., Yang, F., Li, D., and Liu, H., 2017. Statistical monitoring and analysis of energy consumption and emissions during the construction of dao'an Expressway. *Shanghai Highway*, -3-: 17-20. (In Chinese)

Yue, Y., Wang, T., Liang, S., Yang, J., Hou, P., Qu, S., Zhou, J., Jia, X., Wang, H., and Xu, M., 2015. Life cycle assessment of high-speed rail in China. *Transportation Research Part D: Transport and Environment* 41: 367-376.

Zhang, A., Boardman, A.E., Gillen, D., and Waters II, W.G., 2004. Towards Estimating the Social and Environmental Costs of Transportation in Canada, Research Report for Transport Canada, Ottawa, Ontario.

Zhang, A., Wan, Y., and Yang, H., 2019. Impacts of high-speed rail on airlines, airports and regional economies: A survey of recent research. *Transport Policy* 81: A1-A19.

Zhou, Z., and Zhang, A., 2021. High-speed rail and industrial developments: Evidence from house prices and city-level GDP in China. *Transportation Research Part A: Policy and Practice*, forthcoming.

## Appendix

### A. Traffic Density of Various Transportation Modes in Beijing-Shanghai Corridor

Table A Traffic Volume of Various Transportation Mode of B-S Corridor in each OD (Million persons)

| | Beijing-Tianjin | | | | Tianjin-Dezhou | | | | Dezhou-Jinan | | | |
|---|---|---|---|---|---|---|---|---|---|---|---|---|
| | Road | Air | OSR | HSR | Road | Air | OSR | HSR | Road | Air | OSR | HSR |
| 2004 | 19.10 | 4.16 | 35.00 | | 13.18 | 4.65 | 38.33 | | 9.42 | 4.65 | 34.65 | |
| 2005 | 21.34 | 5.85 | 38.54 | | 14.12 | 6.45 | 39.98 | | 11.00 | 6.45 | 35.97 | |
| 2006 | 23.68 | 6.69 | 39.44 | | 15.05 | 7.46 | 43.85 | | 12.58 | 7.46 | 39.18 | |
| 2007 | 26.34 | 7.73 | 36.02 | | 17.59 | 8.59 | 47.28 | | 14.70 | 8.59 | 41.67 | |
| 2008 | 27.46 | 7.80 | 34.82 | | 16.88 | 8.83 | 51.05 | | 12.99 | 8.83 | 44.64 | |
| 2009 | 25.20 | 9.02 | 28.70 | | 16.05 | 10.31 | 51.09 | | 17.59 | 10.31 | 45.95 | |
| 2010 | 24.10 | 10.35 | 30.58 | | 20.51 | 12.12 | 55.35 | | 15.41 | 12.12 | 50.39 | |
| 2011 | 28.05 | 9.69 | 26.58 | 34.03 | 23.45 | 11.27 | 47.81 | 12.99 | 19.34 | 11.27 | 43.49 | 12.91 |
| 2012 | 29.92 | 8.51 | 32.02 | 49.21 | 20.09 | 9.67 | 38.51 | 30.76 | 21.96 | 9.67 | 35.38 | 30.57 |
| 2013 | 22.84 | 8.09 | 22.03 | 58.57 | 23.00 | 9.33 | 38.50 | 38.02 | 20.19 | 9.33 | 36.30 | 37.74 |
| 2014 | 23.67 | 8.22 | 22.86 | 66.08 | 21.33 | 9.40 | 38.07 | 47.27 | 20.35 | 9.40 | 37.63 | 46.95 |
| 2015 | 24.73 | 8.30 | 25.10 | 71.46 | 20.78 | 9.61 | 34.81 | 53.06 | 21.53 | 9.61 | 35.14 | 52.71 |
| 2016 | 23.29 | 8.67 | 22.35 | 79.37 | 20.49 | 9.95 | 32.29 | 58.95 | 21.38 | 9.95 | 34.24 | 58.54 |
| 2017 | 22.88 | 8.82 | 22.47 | 88.33 | 18.22 | 10.15 | 32.33 | 64.20 | 21.23 | 10.15 | 34.55 | 63.93 |

Table A Traffic Volume of Various Transportation Mode of B-S Corridor in each OD (Million persons)

| | Jinan-Yanzhou（Qufu） | | | | Yanzhou（Qufu）-Xuzhou | | | | Xuzhou-Bengbu | | | |
|---|---|---|---|---|---|---|---|---|---|---|---|---|
| | Road | Air | OSR | HSR | Road | Air | OSR | HSR | Road | Air | OSR | HSR |
| 2004 | 13.03 | 4.83 | 39.36 | | 9.42 | 4.83 | 33.84 | | 10.80 | 4.83 | 43.85 | |
| 2005 | 15.22 | 6.61 | 41.14 | | 10.09 | 6.61 | 35.75 | | 9.45 | 6.61 | 45.99 | |
| 2006 | 17.40 | 7.64 | 43.96 | | 10.76 | 7.64 | 38.59 | | 8.10 | 7.73 | 48.90 | |
| 2007 | 21.04 | 8.88 | 39.03 | | 8.29 | 8.88 | 39.70 | | 8.38 | 8.90 | 52.50 | |

| | | | | | | | | | | | | |
|---|---|---|---|---|---|---|---|---|---|---|---|---|
| 2008 | 21.97 | 9.13 | 42.36 | | 9.40 | 9.13 | 41.60 | | 8.67 | 9.14 | 55.56 | |
| 2009 | 23.23 | 10.71 | 42.15 | | 10.34 | 10.71 | 42.00 | | 8.95 | 10.70 | 55.55 | |
| 2010 | 21.89 | 12.79 | 47.24 | | 10.04 | 12.79 | 46.80 | | 10.51 | 12.81 | 64.40 | |
| 2011 | 26.78 | 11.70 | 43.59 | 10.35 | 12.50 | 11.70 | 42.02 | 10.02 | 11.43 | 11.60 | 55.87 | 11.93 |
| 2012 | 28.73 | 9.99 | 39.18 | 25.35 | 13.56 | 9.99 | 36.32 | 24.10 | 11.90 | 9.99 | 47.54 | 29.20 |
| 2013 | 29.81 | 9.67 | 38.99 | 33.02 | 12.96 | 9.67 | 36.11 | 31.37 | 13.09 | 9.67 | 49.61 | 37.80 |
| 2014 | 30.01 | 9.70 | 40.84 | 42.73 | 13.30 | 9.70 | 36.86 | 41.03 | 14.41 | 9.70 | 52.89 | 49.10 |
| 2015 | 29.81 | 9.61 | 37.67 | 49.31 | 13.42 | 9.61 | 33.79 | 47.43 | 15.62 | 9.61 | 50.22 | 56.61 |
| 2016 | 28.53 | 9.95 | 37.34 | 55.64 | 13.69 | 9.95 | 33.99 | 53.01 | 16.62 | 9.95 | 49.39 | 64.40 |
| 2017 | 28.05 | 10.43 | 37.75 | 60.65 | 13.38 | 10.43 | 34.68 | 57.89 | 16.28 | 10.43 | 49.88 | 75.58 |

Table A Traffic Volume of Various Transportation Mode of B-S Corridor in each OD (Million persons)

| | Bengbu-Nanjing | | | | Nanjing-Changzhou | | | | Changzhou-Shanghai | | | |
|---|---|---|---|---|---|---|---|---|---|---|---|---|
| | Road | Air | OSR | HSR | Road | Air | OSR | HSR | Road | Air | OSR | HSR |
| 2004 | 14.32 | 4.83 | 43.65 | | 24.70 | 3.91 | 60.04 | | 33.46 | 3.86 | 61.48 | |
| 2005 | 13.58 | 6.61 | 55.80 | | 37.05 | 5.60 | 62.79 | | 44.52 | 5.51 | 64.99 | |
| 2006 | 12.83 | 7.73 | 59.86 | | 49.40 | 6.64 | 67.03 | | 55.58 | 6.52 | 67.95 | |
| 2007 | 15.12 | 8.90 | 42.30 | | 44.76 | 7.55 | 69.30 | | 62.79 | 7.42 | 69.44 | |
| 2008 | 17.81 | 9.14 | 62.08 | | 59.04 | 7.62 | 74.11 | | 69.27 | 7.51 | 75.12 | |
| 2009 | 19.87 | 10.70 | 58.39 | | 58.46 | 8.79 | 72.83 | | 73.44 | 8.65 | 72.74 | |
| 2010 | 22.76 | 12.81 | 66.37 | | 55.59 | 10.68 | 68.44 | 15.82 | 76.68 | 10.44 | 64.20 | 18.00 |
| 2011 | 26.65 | 11.60 | 56.70 | 12.11 | 43.27 | 9.89 | 49.53 | 39.99 | 63.75 | 9.71 | 41.73 | 43.49 |
| 2012 | 28.64 | 9.99 | 46.60 | 29.81 | 50.47 | 8.94 | 44.49 | 56.20 | 62.79 | 8.81 | 36.96 | 58.68 |
| 2013 | 32.21 | 9.67 | 49.26 | 36.89 | 70.04 | 8.82 | 47.84 | 62.44 | 74.94 | 8.68 | 39.34 | 64.90 |
| 2014 | 33.63 | 9.70 | 54.06 | 47.45 | 76.19 | 8.85 | 51.63 | 70.66 | 82.83 | 8.85 | 42.87 | 74.58 |
| 2015 | 36.73 | 9.61 | 52.06 | 50.95 | 95.00 | 9.61 | 49.94 | 76.75 | 100.05 | 8.76 | 41.94 | 80.32 |
| 2016 | 39.10 | 9.95 | 52.30 | 61.40 | 96.77 | 9.95 | 48.51 | 87.83 | 104.59 | 9.05 | 41.05 | 91.09 |
| 2017 | 40.87 | 10.43 | 53.31 | 73.01 | 80.22 | 9.45 | 48.28 | 101.78 | 103.87 | 9.45 | 41.32 | 103.34 |

## B. Civil Aviation Traffic Volume of B-S Corridor in Each Segment

Table B Civil Aviation Traffic Volume in B-S Corridor in Each Segment from 2011 to 2016

| Year | 2011 | | | 2012 | | | 2013 | | | 2014 | | | 2015 | | | 2016 | | |
|---|---|---|---|---|---|---|---|---|---|---|---|---|---|---|---|---|---|---|
| Segment | Beijing-Shanghai | Shanghai-Tianjin | Nanjing-Beijing | Beijing-Shanghai | Shanghai-Tianjin | Nanjing-Beijing | Beijing-Shanghai | Shanghai-Tianjin | Nanjing-Beijing | Beijing-Shanghai | Shanghai-Tianjin | Nanjing-Beijing | Beijing-Shanghai | Shanghai-Tianjin | Nanjing-Beijing | Beijing-Shanghai | Shanghai-Tianjin | Nanjing-Beijing |
| Shift | 35376 | 11942 | 12049 | 35390 | 10127 | 9130 | 34348 | 9930 | 7170 | 35362 | 10207 | 7740 | 37032 | 11781 | 7874 | 38344 | 11947 | 8407 |
| Traffic Volume (Million persons) | 7.10 | 1.45 | 1.59 | 6.84 | 1.16 | 1.05 | 6.73 | 1.24 | 0.85 | 7.01 | 1.18 | 0.85 | 7.45 | 1.31 | 0.85 | 7.77 | 1.28 | 0.90 |
| Seat (Million) | 8.16 | 1.76 | 1.91 | 8.03 | 1.48 | 1.38 | 7.85 | 1.54 | 1.11 | 8.14 | 1.53 | 1.14 | 8.54 | 1.73 | 1.14 | 8.78 | 1.75 | 1.23 |
| Passenger Load Factor (%) | 86.60 | 84.50 | 83.40 | 85.20 | 81.10 | 76.00 | 85.80 | 83.30 | 76.60 | 86.20 | 80.40 | 74.90 | 87.30 | 80.30 | 74.40 | 88.60 | 80.40 | 73.30 |

Source: "Statistical data on civil aviation of China" (2010-2017)

## C. $CO_2$ Emissions of Operation

Table C1 $CO_2$ Emissions from Diverted Traffic Volume (Ton)

| Year | Beijing-Tianjin | Tianjin-Dezhou | Dezhou-Jinan | Jinan-Yanzhou | Yanzhou-Xuzhou | Xuzhou-Bengbu | Bengbu-Nanjing | Nanjing-Changzhou | Changzhou-Shanghai | Total |
|---|---|---|---|---|---|---|---|---|---|---|
| 2011 | -24993.70 | 19432.95 | 6324.58 | 27337.62 | 91.66 | 11945.90 | 13440.18 | 9471.30 | 5222.00 | 68272.49 |
| 2012 | 470.66 | 52968.97 | 21664.55 | 71982.26 | 13685.55 | 31178.64 | 54260.88 | 33520.07 | -17969.52 | 261762.07 |
| 2013 | -38834.50 | 26212.13 | 1725.76 | 68385.44 | -11000.15 | -334.50 | 21019.86 | -16404.83 | -9371.32 | 41397.88 |
| 2014 | -109786.59 | -19131.45 | -18180.44 | --61197.84 | -35879.92 | -37833.17 | -34697.10 | -52443.11 | -89410.57 | -336164.52 |
| 2015 | -99999.22 | -24853.42 | -26286.12 | 54142.81 | -50474.18 | -62185.01 | -58720.46 | -27300.84 | -80354.59 | -376031.03 |
| 2016 | -112274.15 | -31920.71 | -36057.41 | 41843.76 | -59910.94 | -80383.29 | -83389.74 | -71971.00 | -124125.38 | -558188.87 |
| 2017 | -152045.87 | -67153.04 | -40701.32 | 40936.51 | -90341.69 | -115781.05 | -116187.36 | -87946.72 | -141948.95 | -771169.50 |

Table C2 $CO_2$ Emissions from Generated Traffic Volume (Ton)

| Year | Beijing-Tianjin | Tianjin-Dezhou | Dezhou-Jinan | Jinan-Yanzhou | Yanzhou-Xuzhou | Xuzhou-Bengbu | Bengbu-Nanjing | Nanjing-Changzhou | Changzhou-Shanghai | Total |
|---|---|---|---|---|---|---|---|---|---|---|
| 2011 | 43266.94 | 6310.50 | 7722.44 | 12726.43 | 9130.65 | 244.14 | 1034.08 | 12836.53 | 20224.64 | 113496.34 |
| 2012 | 68802.46 | 18697.03 | 22895.86 | 35289.30 | 27504.64 | 6161.94 | 9990.40 | 37700.92 | 26493.47 | 253536.01 |
| 2013 | 83507.16 | 34135.21 | 24692.17 | 33972.83 | 29340.66 | 14765.28 | 31275.72 | 45932.14 | 78709.58 | 376330.75 |
| 2014 | 72894.14 | 45069.66 | 34775.32 | 49976.23 | 50684.94 | 44977.89 | 61878.64 | 69054.19 | 89970.02 | 519281.03 |
| 2015 | 36506.87 | 37185.72 | 28938.62 | 29746.52 | 39765.21 | 27623.71 | 33793.76 | 85719.92 | 106227.26 | 425507.60 |
| 2016 | 38097.88 | 32326.42 | 27493.64 | 22666.53 | 43120.76 | 22538.06 | 45082.01 | 79974.06 | 110964.35 | 422263.70 |
| 2017 | 42793.84 | 32307.02 | 31362.06 | 29089.70 | 46256.20 | 39627.04 | 65942.01 | 82543.40 | 113322.24 | 483243.50 |